Journal of Applied Polymer Science

Synergistic enhancement of glass fiber and tetrapod-shaped ZnO whisker on the mechanical and thermal behavior of isotactic polypropylene

Songfang Zhao,[1] Lei Cheng,[2] Jinfeng Leng,[1] Lingzhi Guo,[1] Yongju Gao,[3] Yuying Zheng,[2] Duxia Cao[1]

[1]School of Material Science and Engineering, University of Jinan, Jinan, Shandong, 250022, China

[2]College of Materials Science and Engineering, Fuzhou University, Fuzhou, Fujian, 350108, China

[3]Nano Science and Technology Institute, University of Science and Technology of China (USTC), Suzhou, 215123, China

The authors declare that they have no conflict of interest.

Correspondence to: S. Zhao (E-mail: zhaosongfang@163.com), Y. Zheng (E-mail: yyzheng@fzu.edu.cn), or D. Cao (E-mail: mse_caodx@ujn.edu.cn)

ABSTRACT: Improvement of mechanical and thermal properties is always the goal of high-performance general plastic for engineering applications. Herein, isotactic polypropylene/glass fiber/tetrapod-shaped zinc oxide (iPP/GF/T-ZnOw) composites are developed via melt-extrusion on twin-screw extruder. To improve the distribution of T-ZnOw in iPP matrix, T-ZnOw is first modified by various silane coupling agents and its structure is characterized by scanning electron microscopy, Fourier transform infrared spectra, and X-ray diffraction (XRD). The optimized treatment condition is determined via comparison of activation index. The introduction of GF and T-ZnOw could improve the mechanical properties including tensile strength, elastic modulus, flexural strength, flexural modulus, and impact strength, indicating that the surface modification and compatibilizer could enhance the interfacial interaction of iPP/GF/T-ZnOw composites. Moreover, XRD and differential scanning calorimentryresults show that T-ZnOw as a novel β-nucleating agent could induce the formation of β-crystal and the existence of GF counteracts the formation of β-crystal induced by T-ZnOw. © 2016 Wiley Periodicals, Inc. J. Appl. Polym. Sci. **2016**, *133*, 44217.

KEYWORDS: composites; crystallization; extrusion; fibers; thermoplastics

Received 5 May 2016; accepted 21 July 2016

DOI: 10.1002/app.44217

INTRODUCTION

As a result of the versatility, low manufacturing cost, and excellent comprehensive properties, isotactic polypropylene (iPP) has been the major polymeric construction material used in a wide variety of areas including automotive, construction, and other industrial applications.[1–4] Unfortunately, its brittleness at low temperature and notch-sensitive feature limit its further applications.[5,6] Thus, it becomes an urgent and attractive work to improve the mechanical properties of iPP.

As well known, iPP possesses several crystal forms including monoclinic (α), trigonal (β), and orthorhombic (γ). β-form iPP exhibits superior toughness and thermal performance, but its yield strength and stiffness is generally much lower than those of α-form iPP.[7–9] To keep the balance between the strength and toughness, one of the most effective approaches is the combined modification of iPP with various reinforcing fillers as nucleating agents.[10–13] Recently, embedding various fibers (carbon, glass, etc.) in the iPP matrix becomes the major trend because the as-prepared composites exhibit valuable mechanical and thermal properties.[14,15] In our previous work,[16] Kevlar fiber modified with caprolactam was introduced into the iPP matrix, and the as-prepared composites exhibited excellent mechanical and thermal properties. Khanam[17] reported recycled PP composites reinforced by glass fiber (GF) or wood flour, whose stiffness, strength, and hardness was improved. These added fibers act a significant role in the growing of iPP crystals. Tetrapod-shaped zinc oxide whisker (T-ZnOw), as β-nucleating agent, possesses 3D structure with four arms tetragonally connected with a central core with a angle of 109.5°. It has been widely used in various fields including sensor, ultraviolet absorption and polymer composites.[18–20] Mishra[21] reported that T-ZnOw exhibited best performance in improving hydrophobicity of cross-section and the stiffness, because of its special shape. We also found that T-ZnOw as a novel β-nucleating agent could enhance the tensile strength and impact strength of iPP.[22] Three-phase composites have also been studied intensively. Peng used ZnO as a stabilizer and investigated the degradation

Table I. The Formulations of T-ZnOw/GF/iPP Composites in Our Work

	Series 1			Series 2		
iPP	GF	Compatilizer	T-ZnOw	GF	T-ZnOw	Compatilizer
100%	10%	6%	0	10%	1%	0
			1%			3%
			3%			6%
			5%			12%

mechanism of ZnO- GF-unsaturated polyester composite under exposure to a metal halide lamp.[23] Cui employed nano-ZnO treated by KH-550 coupling agent and GFs to improve the mechanical performance and melt flowability of PP.[24] However, there is no work focusing on the effect of T-ZnOw and GF on iPP crystal forms, thus affecting the mechanical and thermal behavior of iPP.

Herein, iPP/GF/T-ZnOw composites are fabricated via melt-extrusion on twin-screw extruder. To improve the distribution of T-ZnOw in iPP matrix, the surface of T-ZnOw is modified by various silane coupling agents. The effects of T-ZnOw, GF and compatibilizer on the crystal forms, mechanical and thermal behavior are investigated. The mechanical properties including tensile strength, elastic modulus, flexural strength, flexural modulus, and impact strength are improved because of the introduction of GF and T-ZnOw. Moreover, the existence of GF counteracts the formation of β crystal induced by T-ZnOw.

EXPERIMENTAL

Materials

iPP (T30s) with melt flow index (MFI) of 3.88 g $(10\ min)^{-1}$ (230 °C, 2.16 kg) is purchased from Fujian Petrochemical. Long GF (T635B) supplied by Taishan Fiberglass Inc has a diameter of 13 μm. Silane coupling agents, named 3-aminnopropyltrimethoxysilane (KH-550) and methacryloxy propyl trimethoxyl silane (KH-570), are purchased from Nanjing Yudeheng Fine Chemical. T-ZnOw is supplied by Chengdu Crystrealm., and the length and diameter of the needles of the T-ZnOw are 10–50 μm and 0.5–5 μm, respectively. The iPP-g-(maleic anhydride/styrene) (iPP-g-MAH/St) with 10.79 wt % of grafting degree is synthesized according to our previous work.[25]

Modification of T-ZnOw

Coupling agents are first dissolved in water/ethanol (10/90; V/V), whose pH value is adjusted in the range of 4–5 by acetic acid. After the complete hydrolyzation of the alkoxyl to hydroxyl, the prebaked T-ZnOw is dispersed in the above mixture, and then the mixture is stirred for some time. Typically, 0.4 g of KH-570 (4 wt % of T-ZnOw) is dissolved in 100 mL water/ethanol (10/90; V/V), and its pH value is kept in the range of 4–5 by acetic acid. After 1 h of hydrolyzation, 10 g of dried T-ZnOw is introduced to the above mixture, and then the mixture is stirred at the stirring rate of 130 r min^{-1} for another 3 h at 40 °C. The modified T-ZnOw is collected by filtration, washed by ethanol, and then dried at 120 °C for 6 h.

Preparation of T-ZnOw/GF/iPP Composites

Modified T-ZnOw, iPP, and iPP-g-MAH/St are premixed in a SHR-5A high-blender (Zhangjiagang Light Industrial Plant) for 1 min, and then poured into the charging barrel, and the long GF is introduced from the middle feed port of a SJSH-30 twin-screw extruder (Shijiazhuang Xingshuo.). The temperature profiles are 175 °C, 195 °C, 210 °C, 210 °C, 210 °C, 195 °C, and 185 °C from hopper to die, and the screw speed is fixed at 90 rpm. All formulations in our work are listed in Table I. The as-prepared composite pellets are dried at 75 °C for 12 h, and various test specimens are prepared using an SZ-550NB injection molding machine (Ningbo Plastic Machine Plant) with 39 MPa of injection pressure. The corresponding injection molding temperatures are set at 190 °C, 200 °C, 220 °C, 185 °C from nozzle to feeding port, respectively.

Characterization

Activation index (AI) is determined as follows: 10 g dried modified T-ZnOw is first introduced into 100 mL deionized water, and then the floated T-ZnOw is collected and dried after 1 h of sonication and 1 h of standing. $AI = m_{\text{floated T-ZnOw}}/m_{\text{total T-ZnOw}} \times 100\%$

The Fourier transform-infrared (FTIR) spectroscopy of the pristine and modified T-ZnOw is performed on Nicolet 360 spectrometer using KBr pellets to further assess whether the reaction has occurred. The mixture of dried T-ZnOw powder and KBr by fast grinding is compressed into transparent slices for FTIR measurement.

The morphology of the T-ZnOw and composites is examined on an environment scanning electron microscope (Philips-FEI XL30) with an accelerating voltage of 20 kV. All samples are coated with a thin layer of gold before characterization.

Wide angle X-ray diffraction (WAXD) spectra are obtained on a Rigaku MiniFlexII X-ray diffractometer employing Cu Ka radiation ($k = 1.54$ Å), and the scanning speed is fixed at 2° min^{-1}.

Differential scanning calorimetry (DSC) measurements are conducted on a NETZSCH STA449C thermal system at a cooling rate of 10 °C min^{-1} from 200 °C to 60 °C and at a heating rate of 10 °C min^{-1} from 60 °C to 200 °C.

The notched impact tests are carried out on a XJJD-5 electronic charpy impact testing machine using a 1.0 J hammer. The tests are conducted according to GB/T 1043, and the blow of the hammer is edgewise. Seven specimens with dimensions of 80 mm × 10 mm × 4 mm and V-shaped gap of 2 mm in the middle, are tested for each sample.

The tensile strength, elastic modulus, flexural strength and flexural modulus are measured on a universal electronic tensile machine according to GB/T 1040-92 and GB/T 9341-2000, respectively. Dumbbell shaped specimens of tensile measurements have length of 155 mm, width of 10 mm and thickness of 4 mm, while the specimens of flexural measurements have

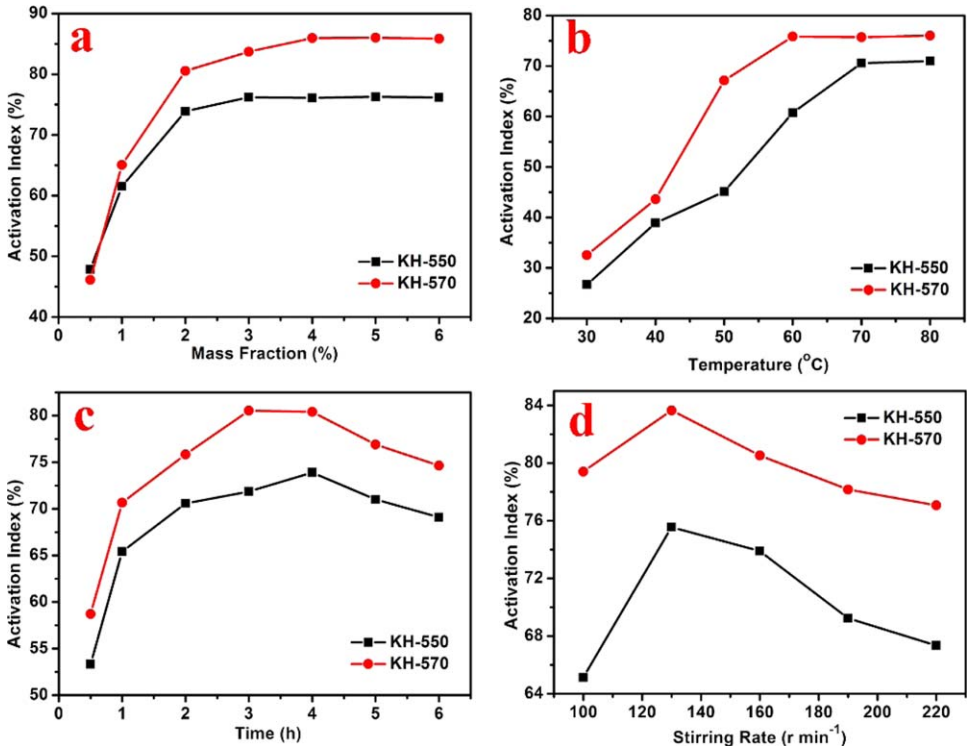

Figure 1. Effects of modification condition on the activation index of T-ZnOw: (a) mass fraction of coupling agents, (b) treatment temperature, (c) treatment time, and (d) stirring rate. [Color figure can be viewed in the online issue, which is available at wileyonlinelibrary.com.]

length of 80 mm, width of 10 mm and thickness of 4 mm. Their crosshead speed is fixed at 50 and 1 mm min^{-1} in tensile and flexural tests, respectively. Each sample is tested five times for average value.

RESULTS AND DISCUSSION

Modification and Characterization of T-ZnOw

To improve the interfacial interaction between the inorganic fillers and polymer matrix, surface treatment is of importance during processing. In order to optimize the modification condition of T-ZnOw, activation index is employed to assess the modification efficiency. In general, pristine T-ZnOw is hydrophilicity and would sink because of its large density of 5.3 g cm^{-3}, while the modified T-ZnOw could float in the water because of its hydrophobicity. Therefore, the modification efficiency could be described by the mass fraction of floating T-ZnOw in water (activation index). The influence of coupling agent content, reaction temperature, time, and stirring rate on the activation index is investigated in Figure 1. From Figure 1(a), it is found that the increase of coupling agent content could endow more T-ZnOw to be modified, resulting in the increase of activation index, while the coupling agent content is beyond certain values, activation index would not be improved because of the formation of multimolecular layers at the surface of T-ZnOw. As described in Figure 1(b), it could be seen that the activation index increases and then reaches a plateau with the increase of temperature. Higher temperature could improve the reaction rate between the hydroxyl of T-ZnOw and coupling agents, however, excessively high temperature would enable adsorbed coupling agents to desorb from the surface of T-ZnOw, which counteracts the positive effect of lower temperature, resulting in no obvious variation of activation index.

Moreover, the treatment time is of importance to achieve modification efficiency. On the one hand, at shorter time, coupling agents could not react completely with the hydroxyl of T-ZnOw, leading to low activation index. On the other hand, the adsorbed coupling agents desorb from the surface of T-ZnOw during long treatment time in Figure 1(c). The influence of stirring rate on the activation index is also investigated in Figure 1(d). The activation index increases first, and then decreases with the increase of stirring rate. Proper stirring rate could improve the reaction between hydroxyl of T-ZnOw and coupling agents, unfortunately, excessively high stirring rate could accelerate the self-polymerization of coupling agents, resulting in the loss of coupling agents. From the above results, KH-570 exhibits better results than KH-550 in improving activation index, because KH-570 has lower polarity of methacryloyloxy group than that of $-NH_2$ in KH-550, which enables modified T-ZnOw by KH-570 to be more hydrophobic, leading to the improvement in activation index. Moreover, the double bond in KH-570 could react with iPP under thermal environment, enhancing the interfacial interaction between T-ZnOw and iPP. Thus, KH-570 is selected as modification agent, and the optimized process condition is as follows: 4 wt % KH-570 of T-ZnOw modifies the T-ZnOw at a temperature of 40 °C, stirring rate of 130 r min^{-1} for 3 h.

The surface morphologies of T-ZnOw modified by KH-550 and KH-570 are shown in Figure 2. It could be seen that T-ZnOw exhibits a 3D shape in the form of four arms pointing out from one core with an angle of ~109.5° with respect to each other. Although the dimensions of these T-ZnOw span up to several

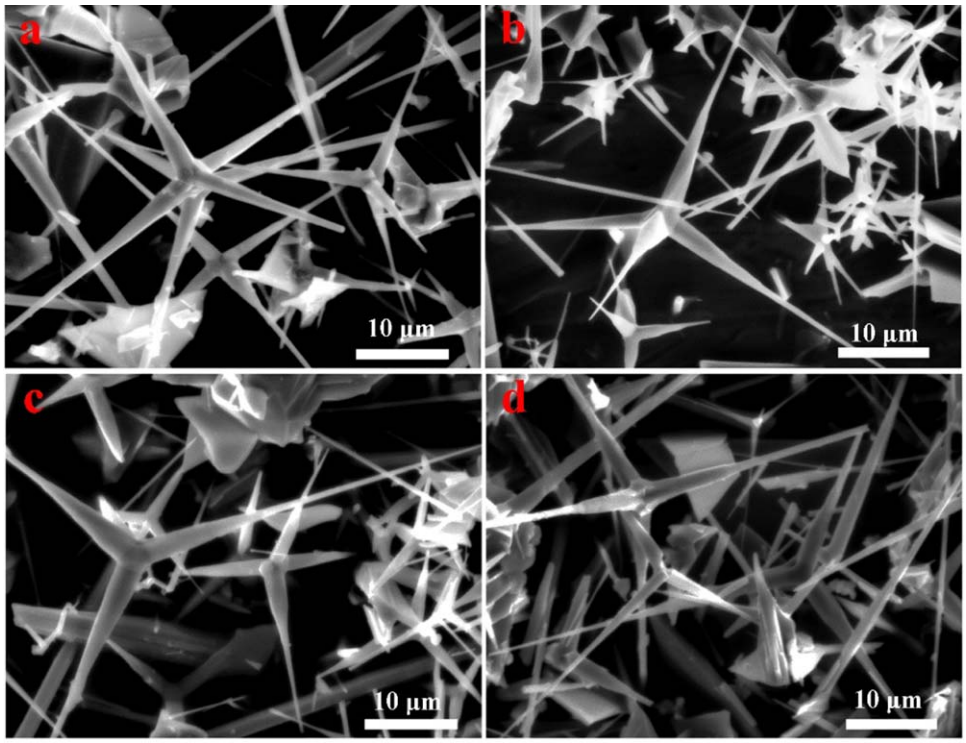

Figure 2. SEM images of T-ZnOw with different modification: (a) unmodified; (b) modified by KH-550 for 3 h; (c) modified by KH-570 for 1 h; and (d) modified by KH-570 for 3 h. [Color figure can be viewed in the online issue, which is available at wileyonlinelibrary.com.]

microns, their arms still possess necessary nanoscale features with aspect ratio ranging from 20 to 30. The unique 3D shape enables them to be well separated from each other without agglomeration. Moreover, it could be observed that these T-ZnOw still maintains their initial 3D structure without destruction after surface modification. However, direct detection of the coupling agents grafted to the T-ZnOw surface using scanning electron microscopy (SEM) microscopy proves to be problematic because of the relative small size of the coupling agents.

In order to confirm the KH-550 and KH-570 grafted to the surface of the T-ZnOw, the FTIR is employed to detect the functional group variations in Figure 3(a). To eliminate the effect of physically absorbed coupling agents on the group variations, Soxhlet extraction is applied to wash the modified T-ZnOw. Compared with these FTIR spectra, the intensity of absorption peak at 3440 cm^{-1} decreases sharply after modification, indicating that -OH of T-ZnOw has been consumed via reaction with KH-550 or KH-570 successfully. The absorption peaks at 2960 and 2850 cm^{-1} are ascribed to the stretching vibrations of the C—H, while the characteristic peaks at 1460 cm^{-1} are attributed to the bending vibrations of the C-H. The absorbed bands ranging from 1040 to 1180 cm^{-1} are ascribed to the stretching vibration of Si—O—Si. Moreover, the absorption peak at 1726 cm^{-1} is assigned to the stretching vibration of the C═O, while the peak at 1633 cm^{-1} is because of the stretching vibration of the C═C.[5,26,27] These indicate that the KH-550 and KH-570 have been grafted to the surface of T-ZnOw, respectively.

Figure 3(b) shows the XRD patterns of raw T-ZnOw and modified T-ZnOw, Seven main diffraction peaks at 2θ values of

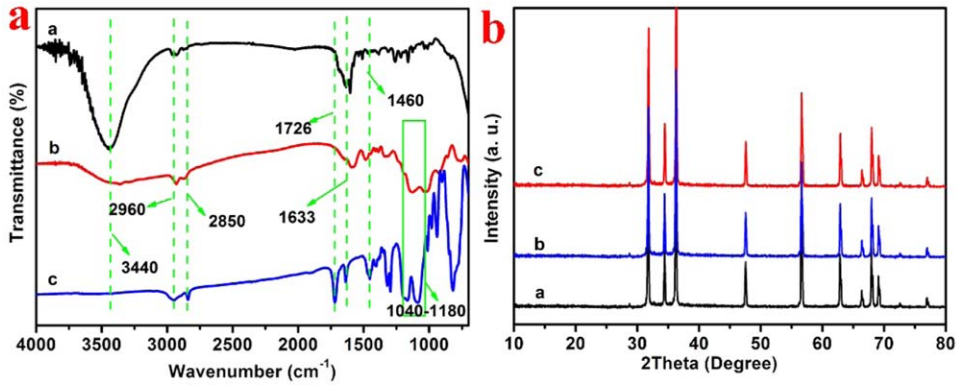

Figure 3. FTIR spectra and XRD spectra of (a) raw T-ZnOw, (b) T-ZnOw modified by KH-550, and (c) T-ZnOw modified by KH-570. [Color figure can be viewed in the online issue, which is available at wileyonlinelibrary.com.]

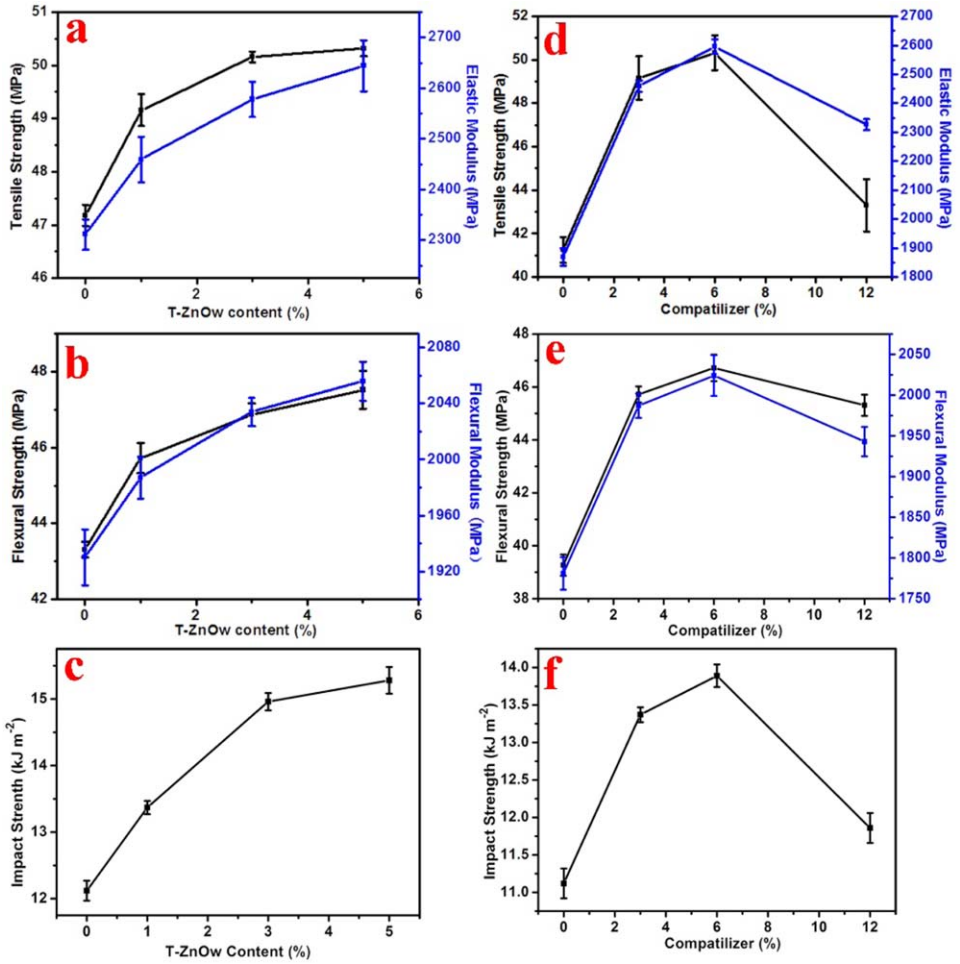

Figure 4. (a–c) Influence of T-ZnOw fraction on the (a) tensile strength and elastic modulus, (b) flexural strength and flexural modulus, (c) impact strength; (d–f) Influence of compatibilizer fraction on the (d) tensile strength and elastic modulus, (e) flexural strength and flexural modulus, (f) impact strength. [Color figure can be viewed in the online issue, which is available at wileyonlinelibrary.com.]

31.8°, 34.4°, 36.3°, 47.6°, 56.6°, 62.8°, and 67.9°, could be indexed to the (100), (002), (101), (102), (110), (103), and (200) crystal planes of T-ZnOw, respectively, indicating a hexagonal structure.[28] Compared with XRD pattern of T-ZnOw, no obvious differences are observed in that of modified T-ZnOw, indicating that coupling agents only modify the surface state without destroying crystal structure.

Mechanical and Thermal Properties of T-ZnOw/GF/iPP Composites

The influence of T-ZnOw and compatibilizer content on the mechanical properties of GF/T-ZnOw/iPP composites is investigated in Figure 4. When the GF and compatibilizer content is fixed at 10 and 6 wt %, it could be seen that tensile strength, elastic modulus, flexural strength, flexural modulus, and impact strength increase firstly and then reach a plateau with the increase of T-ZnOw content in Figure 4(a–c). Under the effect of heat or mechanical stress, polymer radicals are formed from the homolysis of C—C or C—H, and the formed radicals would attack the double bond of KH-570, resulting in the enhancement of interfacial interaction between T-ZnOw and iPP, which is consistent with Madras and Taniike's results.[29,30] Moreover, the framework reinforcement of T-ZnOw enables it to bear partial stress transferred from iPP matrix, resulting in the enhancement of mechanical properties. However, excess T-ZnOw tends to agglomerate and do not further improve mechanical properties.

As can be seen from Figure 4(d–f), the compatibilizer could improve the mechanical properties. The iPP-g-MAH/St compatibilizer possesses numerous of anhydride groups, which could react with the residual —OH of T-ZnOw and -NH_2 of modified GF via esterification and amide reaction, respectively, thus leading to the improvement of interfacial interaction among the iPP, T-ZnOw and GF. However, the mechanical performance decreases when the iPP-g-MAH/St content is beyond 6 wt %, because of the poor mechanical performance of compatibilizer to cause the sacrifice of mechanical properties, which is consistent with the Anastasiadis and Nah's results.[31,32]

The effects of T-ZnOw and GF on the crystallization and melting behavior of iPP are investigated by DSC thermograms, as shown in Figure 5. It could be seen that there is a single peak at 166 °C, corresponding to α-crystal in iPP, while the melting curve of T-ZnOw/iPP composite possesses two melting peaks at

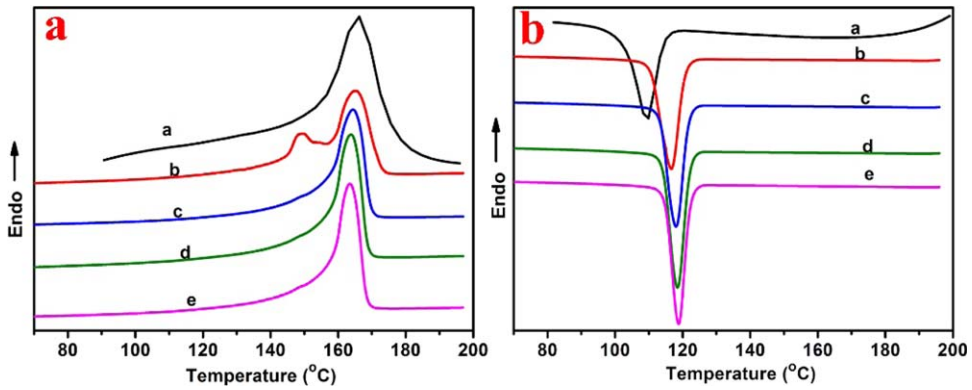

Figure 5. Melting and crystallization behavior of various iPP composites: (a) Pure iPP, (b) T-ZnOw (3 wt %)/iPP composites, (c) GF (10 wt %)/iPP composites, (d) GF (10 wt %)/T-ZnOw (1 wt %)/iPP composites, and (e) GF(10 wt %)/T-ZnOw (3 wt %)/iPP composites. [Color figure can be viewed in the online issue, which is available at wileyonlinelibrary.com.]

165 °C and 149 °C, which are attributed to α-crystal and β-crystal in iPP, respectively. Compared with the melting behavior of pure iPP, the appearance of melting peak at 149 °C and crystal transition at 153 °C indicates that the introduction of T-ZnOw could facilitate the formation of β-crystal during the crystallization process of iPP. On the other hand, there is only one melting peak shifted to 164 °C in the curves of GF/iPP composite, meanwhile, with the addition of T-ZnOw, the melting peak belonging to α-crystal shifts to lower temperature. Interestingly, the introduction of T-ZnOw does not induce the occurrence of β-crystal form in GF/T-ZnOw/iPP composite, which indicates that GF inhibits the occurrence of β-crystal. Moreover, these melting peaks of α-crystal shift towards the lower temperature upon the addition of inorganic fillers. There are two reasons to explain the shifting trend. First, inorganic fillers possess low heat capacity and high thermal conductivity, and then the fillers would preferably be heated faster than iPP, leading to the melting occurrence of polymer molecules adjacent to the fillers at relatively low temperature.[33] Second, the added fillers act as heterogeneous agents to accelerate the crystallization of iPP, resulting in the nonperfect growth of spherocrystal and the decrease of crystallinity in iPP.

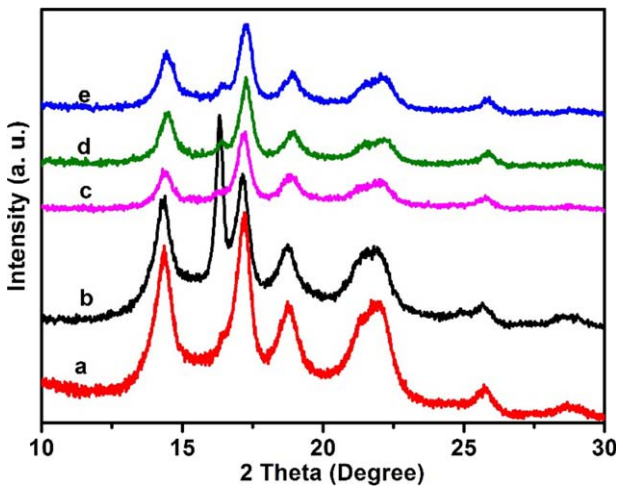

Figure 6. XRD spectra of various iPP composites: (a) Pure iPP, (b) T-ZnOw (3 wt %)/iPP composites, (c) GF (10 wt %)/iPP composites, (d) GF (10 wt %)/T-ZnOw (1 wt %)/iPP composites, and (e) GF(10 wt %)/T-ZnOw (3 wt %)/iPP composites. [Color figure can be viewed in the online issue, which is available at wileyonlinelibrary.com.]

The crystalline behavior of these iPP composites is also investigated in Figure 6(b). It could be observed that the crystallization peak temperature (T_{cp}) and onset temperature (T_{onset}) of pure iPP is 109.2 °C and 118.9 °C, respectively. These T_{cp} and T_{onset} are both improved with the introduction of T-ZnOw and GF, because of the heterogeneous nucleation effect of added inorganic fillers. T-ZnOw and GF enable iPP composites to crystallize at smaller undercooling, inducing the T_{cp} and T_{onset} towards higher temperature, and the increase of crystallization rate. However, the high crystallization rate could generate some defects in iPP spherocrystal during crystallization process, resulting in a decrease of crystallinity.

Structure of T-ZnOw/GF/iPP Composites

As we all know, the physical and mechanical properties of iPP composites are related to their crystalline structure. As shown in Figure 6, the diffraction peaks at 2θ values of 14.1°, 16.9°, 18.5°, 21.2°, and 21.8°, could be indexed to the (110), (040), (130) reflections and overlapping (131) and (111) reflections, respectively, indicating the existence of only α-monoclinic crystal form. In the curve of T-ZnOw/iPP composites, a new peak appears at 2θ values of 16.3°, which corresponds to the (300) reflection of β-hexagonal crystal, indicating the induction of T-ZnOw to β-crystal nucleation.[22] However, in that of GF/iPP composites, the introduction of GF does not change the crystalline structure, but decreases the crystallinity of iPP. Interestingly, the addition of T-ZnOw could not obviously induce the formation of β-hexagonal crystal, because of the inhibition of GF to form β-hexagonal crystal, counteracting the β crystal induction of T-ZnOw.

The cross-sectional morphologies of these composites are shown in Figure 7. It is observed that raw T-ZnOw is pulled out of iPP matrix and some holes are left, indicating poor interfacial interaction between iPP and raw T-ZnOw. Micro-cracks between whisker and iPP would be easily induced upon the applied force, causing the degradation of mechanical properties. After being modified by KH-570, T-ZnOw is tightly embedded in iPP matrix, and the interfaces between T-ZnOw and iPP become

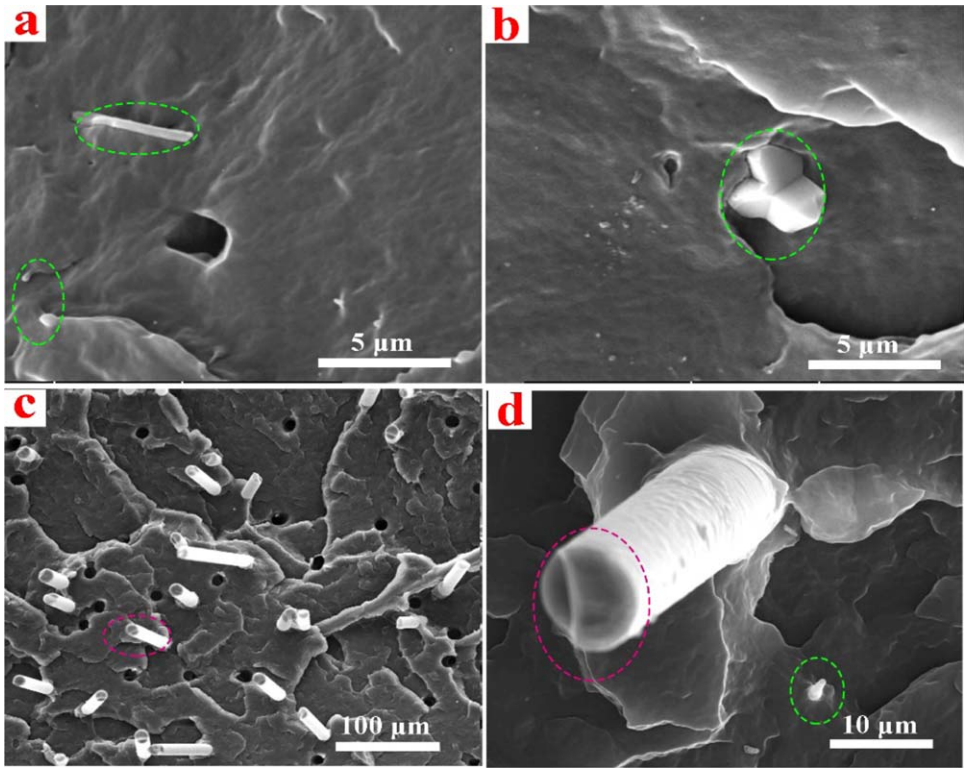

Figure 7. Cross-sectional SEM images of (a) Raw, (b) Modified T-ZnOw/iPP composites, and (c,d) T-ZnOw/GF/iPP composites, composition marked with green ellipse is T-ZnOw (1 wt %), one marked with pink ellipse is GF (10 wt %). [Color figure can be viewed in the online issue, which is available at wileyonlinelibrary.com.]

obscure, implying the enhancement of interfacial adhesion. These contrast results indicate that surface modification could endow the composites with a soft cushioning zone to distribute the stress, improving the mechanical properties. In the T-ZnOw/GF/iPP composites, GF and T-ZnOw is embedded in iPP matrix in staggered forms and enhance the mechanical properties, indicating the synergistic effect of T-ZnOw and GF on the framework of composites. However, the iPP content adhered to the surface of GF is relatively low, indicating the further requirement of enhancing the interfacial interaction among GF and iPP.

CONCLUSIONS

In summary, iPP composites enhanced with T-ZnOw and GF are successfully fabricated via melt-extrusion on twin-screw extruder. To improve the distribution of T-ZnOw in iPP matrix, the optimized modification condition of T-ZnOw by KH-570 is as follows: 4 wt % KH-570 of T-ZnOw, temperature of 40 °C, stirring rate of 130 r min^{-1} for 3 h. While the modified T-ZnOw and GF are introduced into the iPP, the mechanical properties including tensile strength, elastic modulus, flexural strength, flexural modulus, and impact strength, are enhanced, because of that the surface modification and compatibilizer could enhance the interfacial interaction of iPP/GF/T-ZnOw composites. Moreover, these added fillers could increase the crystallization rate and decrease the crystallinity. T-ZnOw as a novel β-nucleating agent could induce the formation of β-crystal, while the existence of GF counteracts the formation of β-crystal induced by T-ZnOw.

ACKNOWLEDGMENTS

This study was funded by the National Natural Science Foundation of China (Grant No. 51301076), the Natural Science Foundation of Fujian Province (Grant No. E0710010) and Fujian Provincial Department of Science and Technology (Grant No. 2007HZ0001-2).

REFERENCES

1. Qin, Y. J.; Xu, Y. H.; Zhang, L. Y.; Zheng, G. Q.; Dai, K.; Liu, C. T.; Yan, X. R.; Guo, J.; Guo, Z. H. *Polymer* **2015**, *70*, 326.
2. Yang, J. H.; Zhang, W.; Ryu, H. J.; Lee, J. H.; Park, D. H.; Choi, J. Y.; Vinu, A.; Elzatahry, A. A.; Choy, J. H. *J. Mater. Chem. A* **2015**, *3*, 22730.
3. Zheng, Z. H.; Liu, Y.; Zhang, L.; Wang, H. Y. *J. Mater. Sci.* **2016**, *51*, 5857.
4. Wang, K.; Guo, M.; Zhao, D. G.; Zhang, Q.; Du, R. N.; Fu, Q.; Dong, X.; Han, C. C. *Polymer* **2006**, *47*, 8374.
5. Zhao, S. F.; Qiu, S. C.; Zheng, Y. Y.; Cheng, L.; Guo, Y. *Mater. Design* **2011**, *32*, 957.
6. Zhang, L. Y.; Qin, Y. J.; Zheng, G. Q.; Dai, K.; Liu, C. T.; Yan, X. R.; Guo, J.; Shen, C. Y.; Guo, Z. H. *Polymer* **2016**, *90*, 18.
7. Rhoades, A. M.; Wonderling, N.; Gohn, A.; Williams, J.; Mileva, D.; Gahleitner, M.; Androsch, R. *Polymer* **2016**, *90*, 67.
8. Luo, F.; Geng, C. Z.; Wang, K.; Deng, H.; Chen, F.; Fu, Q.; Na, B. *Macromolecules* **2009**, *42*, 9325.
9. Zhang, Z. S.; Wang, C. G.; Meng, Y. Z.; Mai, K. C. *Compos. Part A: Appl. Sci.* **2012**, *43*, 189.

10. Sonmez, M.; Georgescu, M.; Valsan, M.; Radulescu, M.; Ficai, D.; Voicu, G.; Ficai, A.; Alexandrescu, L. *J. Appl. Polym. Sci.* **2015**, DOI: 10.1002/app.42163.
11. Bao, R. Y.; Cao, J.; Liu, Z. Y.; Yang, W.; Xie, B. H.; Yang, M. B. *J. Mater. Chem. A* **2014**, *2*, 3190.
12. Prashantha, K.; Soulestin, J.; Lacrampe, M. F.; Claes, M.; Dupin, G.; Krawczak, P. *eXPRESS Polym. Lett.* **2008**, *2*, 735.
13. Wang, Z. J.; Kwon, D. J.; Gu, G. Y.; Kim, H. S.; Kim, D. S.; Lee, C. S.; DeVries, K. L.; Park, J. M. *Compos. Sci. Technol.* **2013**, *81*, 69.
14. Diez-Pascual, A. M.; Naffakh, M. *ACS Appl. Mater. Interfaces* **2013**, *5*, 9691.
15. Abdou, J. P.; Reynolds, K. J.; Pfau, M. R.; Staden, J. V.; Braggin, G. A.; Tajaddod, N.; Minus, M.; Reguero, V.; Vilatela, J. J.; Zhang, S. *Polymer* **2016**, *91*, 136.
16. Zhao, S. F.; Cheng, L.; Guo, Y.; Zheng, Y. Y.; Li, B. M. *Mater. Design* **2012**, *35*, 749.
17. Al-Maadeed, M. A.; Shabana, Y. M.; Khanam, P. N. *Mater. Design* **2009**, *58*, 374.
18. Hu, G.; Ma, Y.; Wang, B. *Mater. Sci. Eng. A* **2009**, *504*, 8.
19. Nie, S. Q.; Zhang, X. L.; Luo, J.; Liu, Y.; Yan, W. *Polym. Compos.* **2015**, DOI: 10.1002/pc.23760.
20. Yuan, F. Y.; Zhang, H. B.; Li, X. F.; Li, X. Z.; Yu, Z. Z. *Compos. Part A: Appl. Sci.* **2013**, *53*, 137.
21. Jin, X.; Deng, M.; Kaps, S.; Zhu, X. W.; Holken, I.; Mess, K.; Adelung, R.; Mishra, Y. K. *Plos One* **2014**, *9*, e106991.
22. Zeng, A. R.; Zheng, Y. Y.; Guo, Y.; Qiu, S. C.; Cheng, L. *Mater. Design* **2012**, *34*, 691.
23. Peng, G. R.; Li, Q. S.; Yang, Y. L.; Wang, H. F. *J. Appl. Polym. Sci.* **2009**, *114*, 2128.
24. Cui, Y. H.; Wang, X. X.; Li, Z. Q.; Tao, J. *J. Vinyl. Addit. Technol.* **2010**, *16*, 189.
25. Zheng, Y. Y.; Zhao, S. F.; Cheng, L.; Li, B. M. *Polym. Bull.* **2010**, *64*, 771.
26. Zhao, S. F.; Zhang, G. P.; Sun, R.; Wong, C. P. *J. Appl. Polym. Sci.* **2014**, DOI: 10.1002/app.40157.
27. Arad-Vosk, N.; Saar, A. *Nanoscale Res. Lett.* **2014**, *9*, 47.
28. Zhou, Z. W.; Peng, W. M.; Ke, S. Y.; Deng, H. *J. Mater. Process. Technol.* **1999**, *89*, 415.
29. Kumar, R.; Madras, G. *J. Appl. Polym. Sci.* **2014**, *90*, 2206.
30. Nakatani, H.; Kurniawan, D.; Taniike, T.; Terano, M. *Sci. Technol. Adv. Mater.* **2008**, *9*, 024401.
31. Chrissopoulou, K.; Anastasiadis, S. H. *Eur. Polym. J.* **2011**, *47*, 600.
32. Hong, C. K.; Kim, M. J.; Oh, S. H.; Lee, Y. S.; Nah, C. *J. Ind. Eng. Chem.* **2008**, *14*, 236.
33. Zhao, S. F.; Gao, Y. J.; Li, J. H.; Zhang, G. P.; Sun, R.; Wong, C. P. *Carbon* **2015**, *95*, 987.